Pré-Publicações do Departamento de Matemática
Universidade de Coimbra
Preprint Number 13–49

DIFFUSION, VISCOELASTICITY AND EROSION: ANALYTICAL STUDY AND MEDICAL APPLICATIONS

E. AZHDARI, J.A. FERREIRA, P. DE OLIVEIRA AND P.M. DA SILVA

Abstract: In this paper diffusion through a viscoelastic biodegradable material is studied. The phenomenon is described by a set of three coupled partial differential equations that take into account passive diffusion, stress driven diffusion and the degradation of the material. The stability properties of the model are studied.

Erodible viscoelastic materials, as biodegradable polymers, have a huge range of applications in medicine to make drug eluting implants. Using the mathematical model the behaviour of a particular ocular drug eluting implant which describes drug delivery into the vitreous chamber of the eye is presented. The model consists of coupled systems of partial differential equations linked by interface conditions. The chemical structure, the viscoelastic properties and the diffusion in the implant as well as the transport in the vitreous are taken into account to simulate the evolution *in vivo* of released drug. The dependence of the delivery profile on the properties of the material are addressed. Numerical simulations that illustrate the interplay between these phenomena are included.

1. Introduction

In the past few decades diffusion through viscoelastic materials has attracted the attention of many researchers ([1, 2, 3, 4, 5]). Apart from the mathematical interest of non Fickian diffusion such research focus is also explained by the increasing practical use of polymers in coatings, packaging, membranes for transdermal drug delivery and more generally in controlled drug delivery ([3, 6]).

It is well known that diffusion through a viscoelastic material does not obey Fick's law. In fact the material opposes a resistance to the Brownian motion of molecules that can be quantified by the stress response to the strain induced by these molecules. Several authors ([7, 8, 9]) have proposed a general model represented by

$$\frac{\partial C_1}{\partial t} = -\nabla . J, \tag{1}$$

Received October 30, 2013.

where C_1 represents drug concentration and J is a modified flux with a stress driven diffusion term defined by

$$J = -D_1 \nabla C_1 - D_v \nabla \sigma, \tag{2}$$

where the stress σ is related with the concentration by some mechanistic model ([10]). In (2) D_1 represents the diffusion coefficient and D_v a viscoelastic parameter which meaning will clarified later.

When the polymer matrix is biodegradable the transport of molecules is not well described by (1)-(2) and a more complex system must be considered. As degradation proceeds, the polymer molecular weight decreases and diffusional paths open through the matrix allowing solved drug molecules to leave the polymeric matrix ([11]). Because of the increasing permeability of the system upon polymer degradation, the constant diffusion coefficient is replaced by a molecular weight dependent diffusion coefficient ([12]) and a reaction term stands for the degradation of drug inside the polymeric matrix is considered (k_1 represents the degradation rate). Equation (1) is then replaced by

$$\frac{\partial C_1}{\partial t} = \nabla.(D_1(M)\nabla C_1 + D_v \nabla \sigma) - k_1 C_1$$

and completed with two other equations: one that describes the mechanistic behaviour of the polymer, that is a relation between stress and strain; another equation which represents the evolution of the material molecular weight as drug concentration changes. One of the contributions of this paper is a theoretical study of this system which leads to a stability restriction with a sound physical meaning: If the Fickian diffusion dominates the non Fickian one the mathematical model is stable. As the material where diffusion occurs is viewed as opposing a barrier to diffusion the theoretical restriction is also a sound physical condition.

Delivering drugs to the vitreous chamber of the eye assumes a crucial role and is a challenging problem due to the presence of various physiological and anatomical barriers. Classical ocular drug delivery systems for posterior segment diseases is systemic or topical.

However none of the these drug delivery systems are effective. In fact systemic delivery is not effective because as the eye has a relatively small size the drug concentration carried by the blood stream is not enough which means that it does not reach the therapeutic window of the drug; with topical delivery just a small fraction of drug reaches the posterior segment of the eye due to physiological barriers. These classical drug delivery systems are being

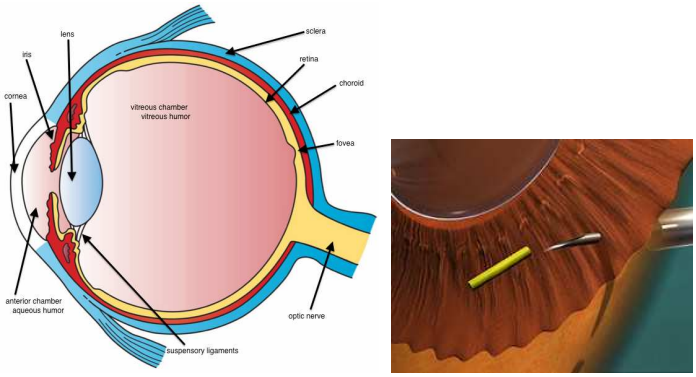

FIGURE 1. Anatomy of the human eye (left) and an ocular implant (right) (http://en.wikipedia.org/wiki/ and http://marcelohosoume.blogspot.pt/2010/10/iluvien-and-future-of-ophthalmic-drug.html).

replaced by direct intravitreal injection or intravitreal implants of drug. As vitreal injections imply several treatments and can cause side effects intravitreal implants have deserved much attention these last years. These polymeric matrices are being used in different medical delivery systems, for example in ocular diseases. In fact there are a number of severe diseases that can affect the vitreous and the retina, which must be treated over long periods of time and where drugs must be maintained in their therapeutic windows (Figure 1). In this paper we will propose a model to simulate intravitreal delivery of drug through viscoelastic biodegradable implants. The model consists of coupled systems of partial differential equations linked by interface conditions. The chemical structure, the viscoelastic properties and the diffusion are taken into account to simulate the evolution of released drug.

Many drugs have a narrow concentration window of effectiveness and may be toxic at higher concentration ([14]), so the ability to predict local drug concentrations is necessary for proper designing of the delivery system. Mathematical models which couple drug delivery from a device with the transport in the living system play a central role because not only they can be used to explain the kinetics of the delivery by describing the interplay of the different phenomena as they quantify the effect of physical and physiological parameters in the delivery trend. Several authors have studied mathematical models to describe transport and elimination of drugs in the vitreous ([14, 15, 16, 17, 18, 19]). However at the best of our knowledge the *in vivo* delivery of drug from a biodegradable implant has not yet been addressed.

Preliminary results were obtained in [20] and [21]. Another aspect we believe is new in our approach is the fact that the theoretical results established are used to obtain physically sound numerical simulations.

The paper is organized as follows. In Section 2 the mathematical model of the diffusion through a viscoelastic biodegradable materials is presented. The qualitative behaviour of the released mass is studied through an *a priori* energy estimate. In Section 3 the medical application is addressed. The geometry of the vitreous chamber of the eye and of the intravitreal implant are described and the mathematical coupled model is presented. Numerical simulations that illustrate the kinetics of the drug release and show the effect of degradation and viscoelasticity are exhibited in Section 4. Finally in Section 5 some conclusions are addressed.

2. Diffusion in a material

In this section the transport of a drug through a biodegradable viscoelastic material is studied. The phenomenon is described by a set of three coupled partial differential equations that take into account passive diffusion, stress driven diffusion and the degradation of the material. The stability properties of the system using the total mass are analysed.

2.1. Mathematical model. We consider a biodegradable viscoelastic material filling a bounded domain $\Omega_1 \subset \mathbb{R}^2$ with boundary $\partial\Omega_1$. A certain amount of drug is dispersed in the polymer. We suppose that when in contact with a penetrant solvent an instantaneous swelling occurs. The drug then dissolves in the solvent and its diffusion through Ω_1 is described by

$$\begin{cases} \dfrac{\partial C_1}{\partial t} = \nabla.(D_1(M)\nabla C_1) + \nabla.(D_v\nabla\sigma) - k_1 C_1 \ \texttt{in}\ \Omega_1 \times (0,T], \\ \dfrac{\partial \sigma}{\partial t} + \dfrac{E}{\mu}\sigma = \overline{E} C_1 \ \texttt{in}\ \Omega_1 \times (0,T], \\ \dfrac{\partial M}{\partial t} + \beta_1 M = \beta_2 C_1 \ \texttt{in}\ \Omega_1 \times (0,T]. \end{cases} \tag{3}$$

In (3) C_1 represents the unknown diffusive concentration of the drug inside the material, for example a polymer, σ is the unknown stress response to the strain exerted by the dissolved drug, and M is the unknown molecular weight of the polymer. The viscoelastic influence in the drug transport is

represented by the term $\nabla.(D_v \nabla\sigma)$ where D_v is a viscoelastic tensor which physical dimension is time. The term $-k_1 C_1$ describes the degradation of drug inside the polymer and the positive constant k_1 is the degradation rate. The viscoelastic term states that the polymer acts as a barrier to the diffusion of the drug: as the drug strains the polymer it reacts with a stress of opposite sign. To account for the increasing permeability of the system upon polymer degradation, the diffusion coefficient is defined by ([12])

$$D_1(M) = D_0 e^{\frac{M_0}{M+M_0}}, \tag{4}$$

where D_0 is the diffusion coefficient of the drug in the non hydrolyzed polymer and M_0 is the initial molecular weight of the polymeric matrix. The second equation in (3) defines the viscoelastic behaviour of the polymer by Maxwell fluid model ([1, 2, 7, 8, 10])

$$\frac{\partial\sigma}{\partial t} + \frac{E}{\mu}\sigma = E\frac{\partial\epsilon}{\partial t}, \tag{5}$$

where E represents the Young modulus of the material, μ is its viscosity and ϵ is the strain produced by the drug molecules. Assuming that the polymer acts as a barrier to the release of the drug, σ and ϵ are of opposite sign, and a minus sign should be considered in the right hand side of (5). To eliminate the strain ϵ in (5) we assume

$$\epsilon(x,t) = k\int_0^t C_1(x,s)ds, \tag{6}$$

where k is a dimensional positive constant ([3]). Replacing (6) in (5) and considering the minus sign in the right hand side of (5) we obtain the second equation in (3) where $\overline{E} = -Ek$. The viscoelastic tensor D_v has a precise physical meaning and for one dimensional model it can be proved that $D_v > 0$ ([22]). In [9, 23, 24] the authors considered $D_v < 0$ and the stress σ and the strain ϵ with the same sign. Even if these arguments are not physically correct from a practical point of view the sign of the viscoelastic term is the same as in our approach. In the third equation of (3) β_1 and β_2 are positive constants that characterize the degradation properties of the material.

System (3) is completed with initial conditions

$$\begin{cases} C_1(x,0) = C_0,\ x \in \Omega_1, \\ \\ \sigma(x,0) = \sigma_0,\ x \in \Omega_1, \\ \\ M(x,0) = M_0,\ x \in \Omega_1, \end{cases} \tag{7}$$

and boundary conditions

$$\begin{cases} C_1(x,0) = 0 \ \texttt{on}\ \partial\Omega_1 \times (0,T], \\ \\ \sigma(x,t) = \sigma_0 e^{-\frac{E}{\mu}t} \ \texttt{on}\ \partial\Omega_1 \times (0,T], \\ \\ M(x,t) = M_0 e^{-\beta_1 t} \ \texttt{on}\ \partial\Omega_1 \times (0,T], \end{cases} \tag{8}$$

where $\partial\Omega_1$ denotes the boundary of Ω_1. The first boundary condition means that the drug is immediately removed as it attains the boundary. The boundary conditions for σ and M have been obtained from the solutions of the second and the third equations of (3), respectively.

2.2. Qualitative behaviour of solution. In this section we study the qualitative behaviour of the energy functional

$$Q(t) = \|C_1(t)\|^2,\ t \geq 0, \tag{9}$$

where $\|.\|$ represents the usual norm in $L^2(\Omega_1)$ which is induced by the corresponding inner product $(.,.)$.

In what follows we drop the argument x and we assume that D_1 and D_v are diagonal matrices where the nonzero entries of D_1, $(D_1)_{ii}$, $i = 1, 2$, satisfy $(D_1)_{ii} \geq \overline{D}_0 > 0, i = 1, 2$, and the nonzero entries of D_v, $(D_v)_{ii}$, $i = 1, 2$, satisfy $|(D_v)_{ii}| \leq \overline{D}_v$. From the second equation of (3) we easily get

$$\sigma(t) = \overline{E} \int_0^t e^{-\frac{E}{\mu}(t-s)} C_1(s) ds + \sigma(0) e^{-\frac{E}{\mu}t},\ t \geq 0,$$

with $\overline{E} = -Ek$ and replacing in the first equation of (3) we obtain for C_1

$$\frac{\partial C_1}{\partial t} = \nabla.(D_1(M)\nabla C_1) - Ek \int_0^t e^{-\frac{E}{\mu}(t-s)} \nabla.(D_v \nabla C_1(s)) ds - k_1 C_1, \tag{10}$$

in $\Omega_1 \times (0,T]$.

As $\frac{1}{2}\frac{dQ}{dt} = (C_1(t), \frac{\partial C_1}{\partial t}(t))$ we deduce, from (10), after multiplying scalarly by $C_1(t)$ and using the first equation of (8) the following

$$\frac{1}{2}\frac{dQ}{dt} = -\left\|\sqrt{D_1(M)}\nabla C_1(t)\right\|^2 + \left(\left(Ek\int_0^t e^{-\frac{E}{\mu}(t-s)}D_v\nabla C_1(s)ds, \nabla C_1(t)\right)\right) - k_1\|C_1(t)\|^2, \tag{11}$$

where $\sqrt{D_1(M)}$ is defined considering the square root of the entrance of $D_1(M)$. In (11) $((.,.))$ denotes inner product of $(L^2(\Omega_1))^2$ and $||.||$ represents the associated norm. From (11) and using Cauchy-Schwarz inequality, we have

$$\frac{1}{2}\frac{dQ}{dt}(t) + \overline{D}_0\left\|\nabla C_1(t)\right\|^2 \leq \frac{Ek}{4\delta^2}\left\|\int_0^t e^{-\frac{E}{\mu}(t-s)}\nabla C_1(s)ds\right\|^2 + \overline{D}_v^2 Ek\delta^2\left\|\nabla C_1(t)\right\|^2 - k_1Q(t), \tag{12}$$

where $\delta \neq 0$. We note that in the application of Cauchy- Schwarz inequality the factors are defined as to be dimensionally sound. From the previous inequality we deduce

$$\frac{1}{2}\frac{dQ}{dt}(t) + k_1Q(t) + (\overline{D}_0 - \overline{D}_v^2 Ek\delta^2)\left\|\nabla C_1(t)\right\|^2 \leq \frac{Ek}{4\delta^2}\int_0^t e^{-2\frac{E}{\mu}(t-s)}ds\int_0^t\left\|\nabla C_1(s)\right\|^2 ds, \tag{13}$$

and then

$$Q(t) + 2k_1\int_0^t Q(s)ds + 2(\overline{D}_0 - \overline{D}_v^2 Ek\delta^2)\int_0^t\left\|\nabla C_1(s)\right\|^2 ds \leq \frac{Ek}{4\delta^2\frac{E}{\mu}}\int_0^t\int_0^s\left\|\nabla C_1(\mu)\right\|^2 d\mu ds + Q(0).$$

If δ^2 is such that

$$\overline{D}_0 - \overline{D}_v^2 Ek\delta^2 > 0$$

we obtain

$$Q(t) + \int_0^t Q(s)ds + \int_0^t\left\|\nabla C_1(s)\right\|^2 ds$$

$$\leq \frac{k\mu}{\min\{1, 2k_1, 2(\overline{D}_0 - \overline{D}_v^2 Ek\delta^2)\}4\delta^2} \int_0^t \int_0^s \left\| \nabla C_1(\mu) \right\|^2 d\mu ds + \frac{1}{\min\{1, 2k_1, 2(\overline{D}_0 - \overline{D}_v^2 Ek\delta^2)\}} Q(0).$$

Finally Gronwall's Lemma leads to

$$Q(t) + \int_0^t Q(s)ds + \int_0^t \left\| \nabla C_1(s) \right\|^2 ds \leq \frac{1}{\min\{1, 2k_1, 2(\overline{D}_0 - \overline{D}_v^2 Ek\delta^2)\}} Q(0) e^{\frac{k\mu}{\min\{1,2k_1,2(\overline{D}_0 - \overline{D}_v^2 Ek\delta^2)\}4\delta^2} t}. \quad (14)$$

This last inequality establishes that $Q(t)$, $\int_0^t Q(s)ds$ and $\int_0^t \left\| \nabla C_1(s) \right\|^2 ds$ are bounded for bounded intervals of time. Inequality (14) can be improved by eliminating the exponential factor in its right hand side. Following [25] we multiply (10) by $e^{\gamma t}$, where γ is a positive constant, obtaining

$$e^{\gamma t} \frac{\partial C_1}{\partial t} = \nabla.(D_1(M)\nabla C_1) e^{\gamma t} - Ek \int_0^t e^{-\frac{E}{\mu}(t-s)} e^{\gamma t} \nabla.(D_v \nabla C_1(s))ds - k_1 e^{\gamma t} C_1 \quad (15)$$

Adding $\gamma e^{\gamma t} C_1(t)$ to both sides of (15) we have

$$\frac{\partial C_{1,\gamma}}{\partial t} = \nabla.(D_1(M)\nabla C_{1,\gamma}) - Ek \int_0^t e^{(\gamma - \frac{E}{\mu})(t-s)} \nabla.(D_v \nabla C_{1,\gamma}(s))ds + \gamma C_{1,\gamma}(t) - k_1 C_{1,\gamma}(t), \quad (16)$$

where $C_{1,\gamma}(t) = e^{\gamma t} C_1(t)$. The last equation leads to

$$\left(\frac{dC_{1,\gamma}}{dt}(t), C_{1,\gamma}(t) \right) + (D_1(M)\nabla C_{1,\gamma}(t), \nabla C_{1,\gamma}(t)) = Ek \left(\left(\int_0^t e^{(\gamma - \frac{E}{\mu})(t-s)} D_v \nabla C_{1,\gamma}(s)ds, \nabla C_{1,\gamma}(t) \right) \right) + (\gamma - k_1)(C_{1,\gamma}(t), C_{1,\gamma}(t)).$$

Using the Cauchy-Schwarz inequality, the first equation of (8) and the notation $Q_\gamma(t) = \|C_{1,\gamma}(t)\|^2$, we easily deduce

$$\frac{d}{dt} Q_\gamma(t) + 2k_1 Q_\gamma(t) - 2\gamma Q_\gamma(t) + 2\overline{D}_0 \left\| \nabla C_{1,\gamma}(t) \right\|^2$$

$$\leq 2\overline{D}_v Ek \int_0^t e^{(\gamma-\frac{E}{\mu})(t-s)} \left\| \nabla C_{1,\gamma}(s) \right\| \left\| \nabla C_{1,\gamma}(t) \right\| ds$$
$$\leq 2\delta^2 \overline{D}_v^2 Ek \left\| \nabla C_{1,\gamma}(t) \right\|^2 + \frac{\beta_\gamma Ek}{2\delta^2} \int_0^t e^{(\gamma-\frac{E}{\mu})(t-s)} \left\| \nabla C_{1,\gamma}(s) \right\|^2 ds,$$

for γ such that $\gamma - \frac{E}{\mu} < 0$ and where β_γ is defined by

$$\int_0^t e^{(\gamma-\frac{E}{\mu})(t-s)} ds < \frac{1}{\frac{E}{\mu} - \gamma} = \beta_\gamma. \tag{17}$$

Since $\left\| C_{1,\gamma} \right\| \leq K_\Omega \left\| \nabla C_{1,\gamma} \right\|$, where K_Ω represents the Poincaré's constant, we have

$$Q_\gamma(t) + 2k_1 \int_0^t Q_\gamma(s) ds + (2\overline{D}_0 - 2\gamma K_\Omega^2 - 2\delta^2 \overline{D}_v^2 Ek) \int_0^t \left\| \nabla C_{1,\gamma}(s) \right\|^2 ds$$
$$\leq Q(0) + \frac{\beta_\gamma Ek}{2\delta^2} \int_0^t \int_0^\eta e^{(\gamma-\frac{E}{\mu})(\eta-s)} \left\| \nabla C_{1,\gamma}(s) \right\|^2 ds d\eta. \tag{18}$$

Changing the order of integration in the double integral in the right hand side of (18) we have

$$Q_\gamma(t) + 2k_1 \int_0^t Q_\gamma(s) ds + (2\overline{D}_0 - 2\gamma K_\Omega^2 - 2\delta^2 \overline{D}_v^2 Ek) \int_0^t \left\| \nabla C_{1,\gamma}(s) \right\|^2 ds$$
$$\leq Q(0) + \frac{\beta_\gamma Ek}{2\delta^2} \int_0^t \int_s^t e^{(\gamma-\frac{E}{\mu})(\eta-s)} d\eta \left\| \nabla C_{1,\gamma}(s) \right\|^2 ds. \tag{19}$$

Computing the interior integral in the right hand side of (19) and considering (17) we obtain

$$Q_\gamma(t) + 2k_1 \int_0^t Q_\gamma(s) ds + (2\overline{D}_0 - 2\gamma K_\Omega^2 - 2\delta^2 \overline{D}_v^2 Ek) \int_0^t \left\| \nabla C_{1,\gamma}(s) \right\|^2 ds$$
$$\leq Q(0) + \frac{\beta_\gamma^2 Ek}{2\delta^2} \int_0^t \left\| \nabla C_{1,\gamma}(s) \right\|^2 ds. \tag{20}$$

As $Q_\gamma(t) = e^{2\gamma t} Q(t)$ we establish

$$Q(t) + 2k_1 \int_0^t e^{-2\gamma(t-s)} Q(s) ds$$

$$+\left(2\overline{D}_0 - 2\gamma K_\Omega^2 - 2\delta^2\overline{D}_v^2 Ek - \frac{Ek}{2\delta^2(\frac{E}{\mu}-\gamma)^2}\right)\int_0^t e^{-2\gamma(t-s)}\left\|\nabla C_1(s)\right\|^2 ds \leq e^{-2\gamma t}Q(0).$$

We now look for γ such that

$$2\overline{D}_0 - 2\gamma K_\Omega^2 - 2\delta^2\overline{D}_v^2 Ek - \frac{Ek}{2\delta^2(\frac{E}{\mu}-\gamma)^2} > 0,$$

with $\dfrac{E}{\mu} - \gamma > 0$.

The parameter δ is arbitrary so we select $\delta = 1$. The function f defined by

$$f(\gamma) = 2\overline{D}_0 - 2\gamma K_\Omega^2 - 2\overline{D}_v^2 Ek - \frac{Ek}{2(\frac{E}{\mu}-\gamma)^2}$$

is a continuous function for $\gamma \in [0, \frac{E}{\mu}[$. We have

$$f(0) = 2\overline{D}_0 - 2\overline{D}_v^2 Ek - \frac{\mu^2 k}{2E}$$

and $\lim\limits_{\gamma\to\frac{E}{\mu}} f(\gamma) < 0$. If we impose

$$\overline{D}_0 - \overline{D}_v^2 Ek - \frac{\mu^2 k}{4E} > 0, \tag{21}$$

the non linear equation

$$f(\gamma) = 0$$

has a positive root in $]0, \frac{E}{\mu}[$.

We have then proved the following result for the energy functional defined in (9).

Theorem 2.1. *If $\overline{D}_0$, $\overline{D}_v$, E, k and μ are such that*

$$\overline{D}_0 - \overline{D}_v^2 Ek - \frac{\mu^2 k}{4E} > 0 \tag{22}$$

then $\exists\gamma \in]0, \frac{E}{\mu}[$ such that

$$Q(t) + \int_0^t e^{-2\gamma(t-s)}Q(s)ds + \int_0^t e^{-2\gamma(t-s)}\left\|\nabla C_1(s)\right\|^2 ds \leq Ce^{-2\gamma t}Q(0),\ t \geq 0, \tag{23}$$

where

$$C = \frac{1}{\min\{1, 2k_1, 2\overline{D}_0 - 2\gamma K_\Omega^2 - 2\overline{D}_v^2 Ek - \frac{Ek}{2(\frac{E}{\mu}-\gamma)^2}\}}.$$

We note that the restriction on the parameters imposed in Theorem 2.1 have a physical meaning. It establishes that the Fickian contribution dominates the non Fickian one, which is a physically sound restriction. In fact if we make a dimensional analysis of (22) for $1D$ case we conclude that all the terms are consistent with dimension $\frac{L^2}{T}$, where L^2 stands for square length and T for time.

To simulate *in vivo* the drug release, the polymeric matrix is coupled with a living system. In this case the Dirichlet boundary conditions (8) should be replaced by a Robin boundary condition of type

$$J.\eta = A_c C_1, \tag{24}$$

where J stands for the flux, η is the exterior unit outward normal to $\partial\Omega_1$ and A_c is a positive constant. The problem to be solved is then the third equation of system (3) and the equation (10) coupled with initial condition (7) and boundary condition in $\partial\Omega_1$

$$\Big(- D_1(M)\nabla C_1(t) + D_v Ek \int_0^t e^{-\frac{E}{\mu}(t-s)} \nabla C_1(s) ds \Big).\eta = A_c C_1(t). \tag{25}$$

The same arguments used in the proof of Theorem 2.1 still hold. In fact equation (10) is of form

$$\frac{\partial C_1}{\partial t}(t) = -\nabla.J(t) - k_1 C_1(t)$$

and multiplying scalarly by C_1 we have

$$\frac{1}{2}\frac{dQ}{dt}(t) = -\Big(J.\eta, C_1\Big)_{\partial\Omega_1} + \Big(J, \nabla C_1\Big) - k_1 \Big\| C_1 \Big\|^2,$$

where

$$\Big(J.\eta, C_1\Big)_{\partial\Omega_1} = \int_{\partial\Omega_1} J.\eta C_1(x,t) dx.$$

From (24) and (25) we obtain, instead of (11), the inequality

$$\frac{1}{2}\frac{dQ}{dt}(t) \leq (J(t), \nabla C_1(t)) - k_1 \|C_1(t)\|^2,$$

and estimate (14) then follows. To eliminate the exponential factor we used the same arguments as in the proof of Theorem 2.1. In this case the existence of $\gamma \in]0, \frac{E}{\mu}[$ such that (23) holds with

$$C = \frac{1}{\min\{1, 2(k_1 - \gamma), 2(\overline{D}_0 - \overline{D}_v^2 Ek - \frac{Ek}{4(\frac{E}{\mu} - \gamma)^2})\}},$$

is guaranteed provided (22) holds and $\frac{E}{\mu} < k_1$.

3. A medical application

In this section we present a medical application of a biodegradable viscoelastic drug eluting implant. As described in Section 1 this type of implant is used for instance in the vitreous chamber of the eye to release drug to the retina. The model presented here describes *in vivo* drug delivery as it couples system (3) with the kinetics of drug in the vitreous chamber of the eye.

3.1. Geometry. The geometrical model of the human eye adopted in the present study is shown in Figure 2 and is based on physiological dimensions ([15]).

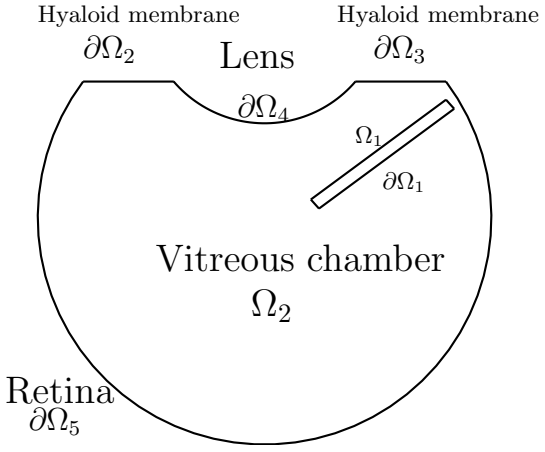

FIGURE 2. Geometry of the vitreous chamber of the human eye (Ω_2), hyaloid membrane ($\partial\Omega_2$, $\partial\Omega_3$), lens ($\partial\Omega_4$), retina ($\partial\Omega_5$), ocular implant (Ω_1) and its boundary ($\partial\Omega_1$).

The vitreous chamber Ω_2 is mainly composed by vitreous humor and it occupies about two-third of the eye. The lens is located behind the iris and is modeled here as an ellipsoid. The hyaloid membrane and the lens separate the anterior chamber and the posterior chamber of the eye from the vitreous chamber. The retina forms the boundary of the vitreous on the posterior surface and is modeled as a spherical surface with a radius of 9.1 mm. The intravitreal implant Ω_1 is placed into the vitreous, as shown in Figure 2, and it is geometrically represented by a cylinder with radius 0.023 mm and height 0.6 mm.

3.2. Mathematical model. The implant Ω_1 containing dispersed drug is placed into the vitreous, near the retina (Figure 2). The drug is released in a controlled manner through the vitreous which is a porous media, and its target is the retina affected by an inflammatory process.

The diffusion-reaction equation that describes the drug dynamics in the polymeric implant is represented by system (3), coupled with initial conditions (7). We couple with this system the drug dynamics in the vitreous, where the diffusion of drug occurs from the polymer towards the vitreous and the retina. Mass transport in the vitreous is described by diffusion and convection. Convection is due to the steady permeation of the aqueous humor through the vitreous, and diffusion is driven by the concentration gradient ([17]). To simulate the dynamics of the drug in the vitreous we use a diffusion reaction equation, where the permeation velocity of the aqueous humor is given by Darcy's law ([14, 15, 18, 19, 26, 27]), as follows:

$$\frac{\partial C_2}{\partial t} + \nabla.(C_2\mathbf{v}) - \nabla.(D_2\nabla C_2) = 0 \,\texttt{in}\, \Omega_2 \times (0,T], \tag{26}$$

and

$$\begin{cases} \mathbf{v} = -\dfrac{K}{\mu_1}\nabla p \,\texttt{in}\, \Omega_2 \times (0,T] \\ \nabla.\mathbf{v} = 0 \,\texttt{in}\, \Omega_2 \times (0,T] \end{cases}. \tag{27}$$

In equation (26) C_2 represents the concentration of the drug in the vitreous, D_2 is the diffusion coefficient of the drug in the vitreous and $\mathbf{v}$ is the velocity of aqueous humor permeation given by (27). In this last system K is the permeability of the vitreous and μ_1 is the viscosity of the permeating aqueous humour ([17]). The term $\dfrac{K}{\mu_1}$ is referred to as the hydraulic conductivity.

Equations (3), (26) and (27) are completed with initial conditions represented by

$$\begin{cases} C_1(x,0) = C_0 \,\texttt{in}\, \Omega_1, \\ \sigma(x,0) = \sigma_0 \,\texttt{in}\, \Omega_1, \\ M(x,0) = M_0 \,\texttt{in}\, \Omega_1, \\ C_2(x,0) = 0 \,\texttt{in}\, \Omega_2. \end{cases} \tag{28}$$

Boundary conditions of different types will be used in the model:

- Boundary conditions for the pressure:

$$p = 2000 \,\texttt{on}\ \partial\Omega_2 \cup \partial\Omega_3 \times (0,T],$$

$$p = 1200 \,\texttt{on}\ \partial\Omega_5 \times (0,T].$$

We note that $\partial\Omega_2 \cup \partial\Omega_3$ represents the hyaloid membrane and $\partial\Omega_5$ represents the retina. The two previous values of the pressure that we considered correspond to the intra ocular pressure in the anterior chamber near the lens and the pressure of the blood system, respectively.

- Boundary conditions for the drug concentration:

$$C_2 = 0 \,\texttt{on}\ \partial\Omega_5 \times (0,T],$$

$$(-D_2\nabla C_2 + \mathbf{v}C_2).\eta = 0 \,\texttt{on}\ \partial\Omega_2 \cup \partial\Omega_3 \cup \partial\Omega_4 \times (0,T].$$

- Wall conditions for the velocity:

$$\mathbf{v} = 0$$

on the boundary $\partial\Omega_4$ of the vitreous chamber Ω_2 and on the boundary of the implant $\partial\Omega_1$ (Figure 2).

- Interface boundary conditions for the flux of drug concentration:

$$(-D_1(M)\nabla C_1 - D_v\nabla\sigma).\eta = A_c(C_1 - C_2) \,\texttt{on}\ \partial\Omega_1 \times (0,T],$$

where A_c is the permeability constant and η is the unit exterior normal to $\partial\Omega_1$.

3.3. Numerical simulations. In this section we illustrate the behaviour of drug concentration in the implant and in the vitreous. In the case the values of the constants are not available in the literature, we use values that make physical sense but that may not correspond to the exact characteristics of the intravitreous implants in the market. For this reason the present study has for the moment mainly a qualitative character.

The numerical simulations have been obtained with $C_0 = 1.7887 \times 10^{-6}$, $M_0 = 0.5 \times 10^{-6}$ and $\sigma_0 = 0.5 \times 10^{-6}$, that represent the initial drug concentration, initial stress and the initial molecular weight in the implant, respectively. The units used for concentration are mol/mm^3. For the other variables the units are selected such that the equations are dimensionally correct.

The diffusion coefficient of the drug in the implant is defined considering $D_0 = 1 \times 10^{-11} I_2$ in (4), where I_2 is the identity matrix and its diffusion coefficient in the vitreous is defined by $D_2 = 1 \times 10^{-8} I_2$. We recall that the diffusion coefficient in the polymer will increase as the molecular weight decreases that is as degradation occurs. The following values for the parameters have been considered:

$$k_1 = 1{\times}10^{-10},\ \beta_1 = 5{\times}10^{-4},\ \beta_2 = 1{\times}10^{-9},\ \mu = 2{\times}10^{-4},\ E = 1{\times}10^{-7},\ k = 1,$$

and

$$A_c = 5 \times 10^{-5},\ D_v = 1 \times 10^{-11} I_2,\ \mu_1 = 0.7,\ \rho = 970,\ K = 0.7 \times 8.4 \times 10^{-8}.$$

The units of the previous parameters are such that the equations are dimensionally correct when concentrations are considered in mol/mm^3 as previously indicated. We observe that the parameters which are used in the numerical simulations are in agreement with condition (22) imposed in Theorem 2.1.

In Figure 3 the drug concentration at time $t = 5\,min$ and $t = 1\,h$ are presented. It can be observed that as time evolves the drug is released and less drug concentration is inside the implant. We remark that the maximum concentration for $t = 5\,min$ is higher than the maximum concentration at $t = 1\,h$.

The pressure in the vitreous chamber is showed in Figure 4. The evolution of the pressure from the top ($p = 2000\,Pa$) to the boundary of the vitreous chamber that is in contact with the retina ($p = 1200\,Pa$), can be observed.

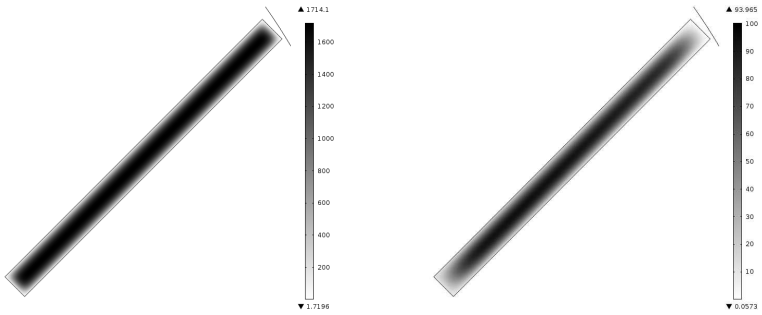

FIGURE 3. Drug concentration in the implant at $5\,min$ (left) and $1\,h$ (right).

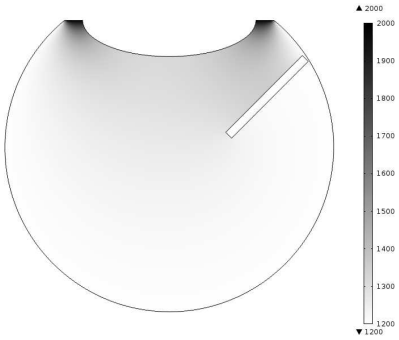

FIGURE 4. Steady pressure in the vitreous chamber.

In Figure 5 the drug concentration in the vitreous chamber is plotted for $t = 5\,min$ and $t = 1\,h$.

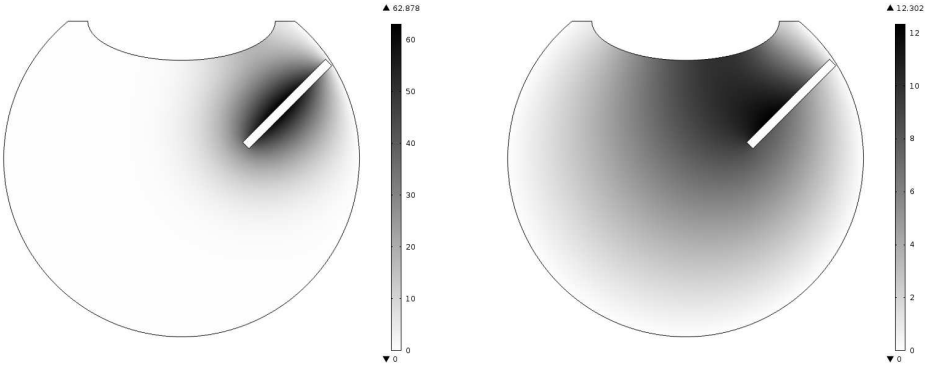

FIGURE 5. Drug concentration in the vitreous chamber at $5\,min$ (left) and $1\,h$ (right).

During the first instants of the delivery process, no drug is observed in the vitreous, except near the ocular implant, and as time increases more

drug concentration is available to diffuse. For a better understanding of the qualitative behaviour of the drug concentration in the vitreous chamber, we present in Figure 6, the plot of drug concentration *vs* time inside the implant and the vitreous chamber. It can be observed that the drug concentration in the vitreous chamber increases until it attains a maximum value at $t = 30\,min$; for $t > 30\,min$ the drug concentration decreases until no drug concentration is present in the ocular implant. This qualitative behaviour is in agreement with medical data, establishing that for a duration of T units of time the maximum concentration of drug is attained for $\overline{T}$, where $\frac{T}{4} < \overline{T} < \frac{T}{3}$.

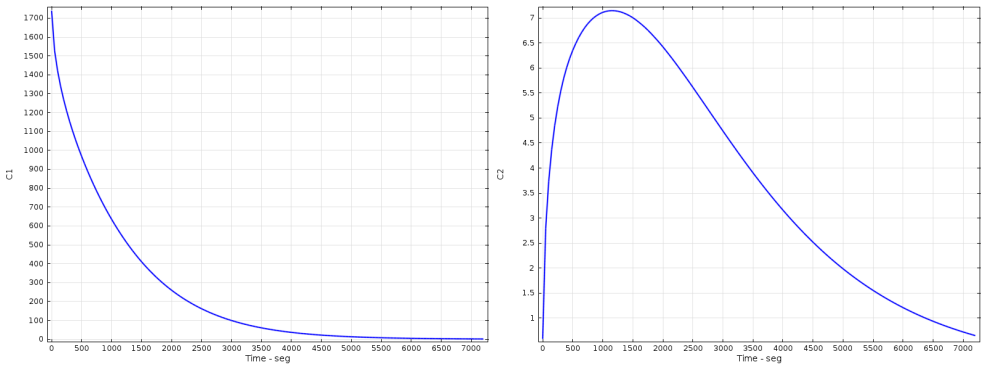

FIGURE 6. Drug concentration in the implant (left) and in the vitreous chamber (right) during two hours.

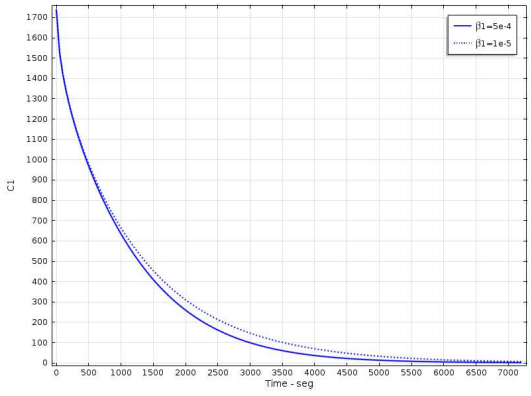

FIGURE 7. Drug concentration in the implant at $t = 2h$ - influence of degradation rate $\beta_1 = 5 \times 10^{-4}$ (down line) and $\beta_1 = 1 \times 10^{-5}$ (top line).

In Figure 7 the influence of the degradation rate is illustrated: a smaller value of β_1 leads to a slower degradation process and consequently more concentration is observed inside the polymeric implant.

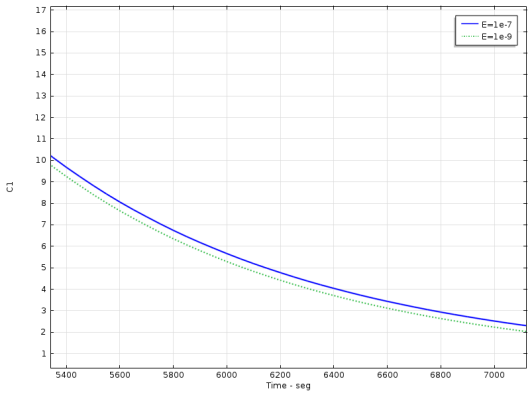

FIGURE 8. Drug concentration at a point of the boundary of the implant around $t = 110\,min$ - influence of E, $E = 1 \times 10^{-7}$ (top line) and $E = 1 \times 10^{-9}$ (bottom line).

In Figure 8 the influence of Young's modulus is illustrated. As expected the increase of Young's modulus, E, delays the drug release and consequently more drug concentration is observed inside the polymer. In fact as crosslinking density is proportional to E, the large is this parameter, the more stiff is the material and a more significant barrier difficults the release of drug.

In Figure 9 the influence of diffusion D_0 on the mass of drug delivered in the vitreous is shown. It is observed that as D_0 increases the mass increases because the diffusion process becomes faster.

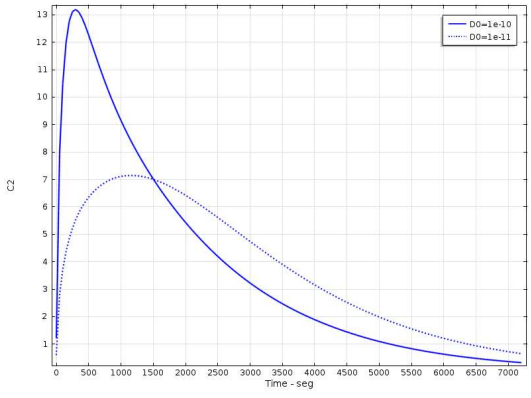

FIGURE 9. Influence of parameters D_0 on the mass of drug in the vitreous.

In Figure 10 we observe that increasing the diffusion coefficient of drug in the vitreous, the mass of drug is also increasing as expected.

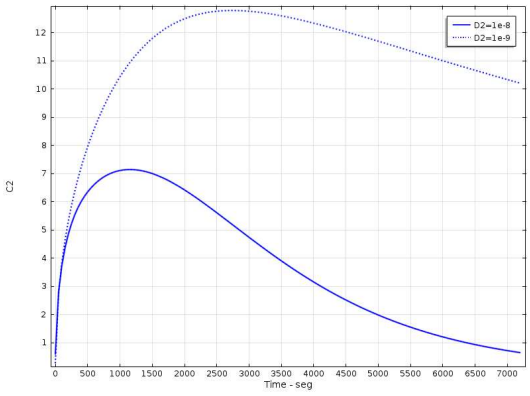

FIGURE 10. Influence of parameter D_2 in the mass of drug released in the vitreous.

4. Conclusion

A coupled model to simulate *in vivo* drug delivery from an intravitreal viscoelastic biodegradable implant has been developed. The whole process is described by a set of partial differential equations that take into account passive diffusion, convection resulting from the permeation of aqueous humor, stress driven diffusion and the degradation of the polymer. At the best of our knowledge the dynamics of diffusion has not been described so far in the literature considering the simultaneous interplay between mechanical, physical and chemical effects. The numerical simulations show qualitative agreement with the physical expected behavior. The model clarifies the large influence of the degradation parameter in sustained drug delivery. The viscoelastic properties of the polymeric implant are also shown to be an effective control mechanism to delay or to speed up the release of drug.

Mathematical modeling is a unique tool to explain transport mechanisms, and to help in implant design, avoiding expensive and extensive experimentation. In future work physical values for all the parameters of the model should be retrieved. Also more realistic mechanical models will be considered and the heterogeneous structure of the vitreous, that is characteristic of elderly patients, should be taken into account.

Acknowledgements

This work was partially supported by the Centro de Matemática da Universidade de Coimbra (CMUC), funded by the European Regional Development Fund through the program COMPETE and by the Portuguese Government through the FCT - Fundação para a Ciência e Tecnologia under the project PEst-C/MAT/UI0324/2013, grant number SFR/BD/33703/2009 and project UTAustin/MAT/0066/2008.

References

[1] D.S. Cohen, A.B. White, JR., and T.P. Witelski, Shock formation in a multidimensional viscoelastic diffusive system, SIAM Journal of Applied Mathematics 55 (1995) 348–368.
[2] D.S. Cohen, A.B. White, JR, Sharp fronts due to diffusion and viscoelastic relaxation in polymers, SIAM Journal of Applied Mathematics 51 (1991) 472–483.
[3] D.A. Edwards, Non-Fickian diffusion in thin polymer films, Journal of Polymer Science: Part B: Polymer Physics 34 (1996) 981–997.
[4] D.A. Edwards, D.S. Cohen, A mathematical model for a dissolving polymer, AIChE J. 18 (1995) 2345–2355.
[5] D.A. Edwards, R.A. Cairncross, Desorption overshoot in polymer-penetrant systems, Asymptotic and computational results. SIAM Journal of Applied Mathematics 63 (2002) 98–115.
[6] J.A. Ferreira, P. de Oliveira, P.M. da Silva, J.N. Murta, Numerical simulation of aqueous humor flow: from healthy to pathologic situations, Preprint 12-17, Department of Mathematics of University of Coimbra, 2013 (submitted).
[7] J.A. Ferreira, P. de Oliveira, P.M. da Silva, Reaction-diffusion in viscoelastic materials, Journal of Computational ana Applied Mathematics 236 (2012) 3783–3795.
[8] J.A. Ferreira, P. de Oliveira, P.M. da Silva, Analityc and numerics of drug tracking, Journal of Computational ana Applied Mathematics 236 (2012) 3572–3583.
[9] J.A. Ferreira, P. de Oliveira, P.M. da Silva, L. Simon, Flux tracking in delivery polymeric systems, Applied Mathematical Modelling 35 (2011) 4684–4696.
[10] H.F. Brinson, L.C. Brinson, Polymer Engineering Science and Viscoelasticity: An Introduction, Springer, 2008.
[11] G. Perale, P. Arosio, D. Moscatelli, V. Barri, M. Müller, S. Maccagnan and M. Masi, A new model of resorbable device degradation and drug release: transient 1-dimension diffusional model, Journal of Controlled Release 136 (2009) 196–205.
[12] J. Siepmann, A. Göpferich, Mathematical modeling of bioerodible polymeric drug delivery systems, Advanced Drug Delivery Reviews 48 (2001) 229–247.
[13] S. Shaw, J.R. Whiteman, Adaptative space-time finite element solution for Volterra equations arising in viscoelasticity problems, Journal of Computational and Applied Mathematics 125 (2000) 337–345.
[14] M.S. Stay, J. Xu, T.W. Randolph, and V.H. Barocas, Computer simulation of convective and diffusive transport of controlled-release drug in the vitreous humor, Pharmaceutical Research 20 (2003) 96–102.
[15] R.K. Balachandran and V.H. Barocas, Computer modeling of drug delivery to the posterior eye: effect of active transport and loss to choroidal blood flow, Pharmaceutical Research 25 (2008) 2685–2696.

[16] R.K. Balachandran and V.H. Barocas, Finite element modeling of drug distribution in the vitreous humor of the rabbit eye, Annals of Biomedical Engineering 25 (1997) 303–314.
[17] J. Kathawate and S. Acharya, Computational modeling of intravitreal drug delivery in the vitreous chamber with different vitreous substitutes, International Journal of Heat and Mass Transfer 51 (2008) 5598–5609.
[18] D. Cox, R.A.J. Phipps, B. Levine, A. Jacobs and D. Fowler, Distribution of phencyclidine into vitreous humor, Journal of Analytical Toxicology 31 (2007) 537–539.
[19] C.W. Misner, K.S. Thorne and J.A. Wheeler, Computer modeling of drug delivery to the posterior eye: effect of active transport and loss to choroidal blood flow, Freeman, San Francisco, 1970.
[20] E. Azhdari, J.A. Ferreira, P. de Oliveira, P.M. da Silva, Analytical and numerical study of diffusion through biodegradable viscoelastic materials, Proceedings of the 13th International Conference on Computational and Mathematical Methods in Science and Engineering, CMMSE 2013, I (2013), 174–184.
[21] E. Azhdari, J.A. Ferreira, P. de Oliveira, P.M. da Silva, Drug delivery from an ocular implant into the vitreous chamber of the eye, Proceedings of the 13th International Conference on Computational and Mathematical Methods in Science and Engineering, CMMSE 2013, I (2013) 185–195.
[22] J.A. Ferreira, M. Grassi, E. Gudino, P. de Oliveira, A new look to non-Fickian diusion, Preprint n. 13-05, Department of Mathematics of Universidade de Coimbra, 2013 (submitted).
[23] Q. Liu, X. Wang, D. De Kee, Mass transport through swelling membranes, International Journal of Engineering Science 43 (2005) 1464–1470.
[24] Q. Liu, D. De Kee, Modeling of diffusion through polymeric membranes, Rheolgica Acta 44 (2005) 287–294.
[25] V. Thomée and L.B. Wahlbin, Long-time numerical solution of a parabolic equation with memory, Mathematics of Computation 62 (1994) 477–496.
[26] R. Avatar, D. Tandon, A mathematical analysis of intravitreal drug transport, Journal of Pharmaceutical Research 7 (2008) 867–877.
[27] N. Haghjou, M.J. Abdekhodaie, Y.L. Cheng. M. Saadatmand, Computer modeling of drug distribution after intravitreal administration, W.A.S. Engineering and Tecnology 53 (2011) 706–716.

E. Azhdari
CMUC-Department of Mathematics, University of Coimbra, Apartado 3008, 3001-454 Coimbra, Portugal

E-mail address: ebrahim@mat.uc.pt

J.A. Ferreira
CMUC-Department of Mathematics, University of Coimbra, Apartado 3008, 3001-454 Coimbra, Portugal

E-mail address: ferreira@mat.uc.pt
URL: http://www.mat.uc.pt/~ferreira

P. de Oliveira
CMUC-Department of Mathematics, University of Coimbra, Apartado 3008, 3001-454 Coimbra, Portugal

E-mail address: poliveir@mat.uc.pt

P.M. da Silva
Instituto Politécnico de Coimbra, ISEC, DFM, Rua Pedro Nunes, 3030-199 Coimbra, Portugal. CMUC.
E-mail address: pascals@isec.pt